HHS Public Access

Author manuscript

Biomed Pharmacother. Author manuscript; available in PMC 2022 May 10.

Published in final edited form as:

Biomed Pharmacother. 2020 December ; 132: 110865. doi:10.1016/j.biopha.2020.110865.

Selective internal radiation therapy of hepatic tumors: Morphologic and functional imaging for voxel-based computer-aided dosimetry

Andrea Skanjeti[a,b,*], **Nicolas Magand**[c], **Didier Defez**[d], **Jeremie Tordo**[a], **Agnes Rode**[c], **Anne Frederique Manichon**[c], **François Hallouard**[e], **Caroline Clave-Darcissac**[e], **Anthony Dhomps**[a], **Danyelle M. Townsend**[f], **Domenico Rubello**[g], **Francesco Giammarile**[h]

[a]Nuclear Medicine Department, Hospices Civils de Lyon, 165 Chemin du Grand Revoyet, 69310 Pierre-Bénite, France

[b]EA 3738, Université Claude Bernard Lyon 1, 165 Chemin du Grand Revoyet, 69310 Pierre-Bénite, France

[c]Radiology Department, Hôpital de la Croix-Rousse, Hospices Civils de Lyon, 103 Grande Rue de la Croix-Rousse, 69004 Lyon, France

[d]Medical Physics Department, Centre Hospitalier Lyon Sud, Hospices Civils de Lyon, 165 Chemin du Grand Revoyet, 69310 Pierre-Bénite, France

[e]Radiopharmacy Unit, Pharmacy Department, Groupement Hospitalier Sud, Hospices Civils de Lyon, 165 Chemin du Grand Revoyet, 69310 Pierre-Bénite, France

[f]Drug Discovery and Pharmaceutical Sciences, Medical University of South Carolina, 70 President St, Charleston, SC 29425, USA

[g]Nuclear Medicine Unit, Santa Maria della Misericordia Hospital, Viale Tre Martiri, 140, 45100 Rovigo, Italy

[h]Division of Human Health, International Atomic Energy Agency, Wagramer Str. 5, 1220 Vienna, Austria

Abstract

Introduction: Selective Internal Radiation Therapy (SIRT) is used for the treatment of hepatic tumors. The aim of this retrospective study was to compare two dosimetric approaches based on ^{99m}Tc-MAA SPECT/CT and ^{90}Y PET/CT, using Simplicit^{90}Y™ *versus* the supplier suggested method of activity calculation.

[*]Corresponding author at: Nuclear Medicine Department, Hospices Civils de Lyon, EA 3738, Université Claude Bernard Lyon 1, 165 Chemin du Grand Revoyet, 69310 Pierre-Bénite, France. askanjeti@gmail.com (A. Skanjeti).

Declaration of Competing Interest

The authors report no declarations of interest

Appendix A. Supplementary data

Supplementary material related to this article can be found, in the online version, at doi:https://doi.org/10.1016/j.biopha.2020.110865.

Material and methods: A total of 19 patients underwent 21 SIRT after baseline angiography and 99mTc-MAA SPECT/CT, followed by 90Y PET/CT. Overlap between 99mTc-MAA and 90Y-microspheres was quantified with different thresholds isocontours. The perfused volume and tumor absorbed dose were estimated using Simplicit90Y™ based on SPECT/CT and PET/CT, then compared with the supplier suggested method. These data were related to overall survival to evaluate their prognostic impact.

Results: The overlap between PET/CT and SPECT/CT was dependent on thresholds, decreasing with an increasing threshold. The overlap between the 99mTc-MAA and 90Y-microspheres biodistributions versus the tumor distribution on morphological imaging was suboptimal, in particular for small tumor volume. The tumor absorbed dose estimated after 90Y PET/CT was not different from tumor absorbed dose estimated after SPECT/CT. The Perfused lobe absorbed dose was significantly lower while the volume of the perfused lobe was significantly higher when estimated by Simplicit90Y™ compared to the supplier suggested conventional approach. A statistical parameter based on overlap between tumor and 90Y-microspheres distribution as well as tumoral dosimetry was significantly related to the overall survival.

Conclusion: Post-treatment imaging remains paramount to estimate the irradiation dosimetry, due to an imperfect overlap. The perfused volume could be estimated from functional imaging, given its impact on dosimetry. Finally, survival seems related to tumoral overlap and dosimetry.

Keywords

SIRT; Hepatic tumors; Voxel-based dosimetry; Survival

1. Introduction

Glass or resin ^{90}Yttrium (^{90}Y) microspheres are commercially available for the Selective Internal Radiation Therapy (SIRT) of hepatocellular carcinoma (HCC) and liver metastatic infiltrations in case of extrahepatic tumors. The purpose of this treatment is to perform a focal administration, using a catheter in the hepatic arterial flow, of highly radioactive ^{90}Y resin-bounded microspheres or ^{90}Y glass matrix-embedded microspheres. Then, as the tumor vascularization is naturally selective for the arterial blood, and the portal blood vascularizes the healthy liver parenchyma, a selective irradiation of the tumor is achieved.

The advantages of these intra-arterial radioactive compounds include the high delivered absorbed doses to target volumes with relatively low toxicity profile, the ability to target the to-be-treated area (the whole liver, a liver lobe, or a segment), and the possibility to combine other therapy modalities. The disadvantages are mainly due to the radioprotection constraints and the limitation to hepatic treatment only [1]. After a baseline angiography and the administration of ^{99m}Tc-MAA, a Single Photon Emission Computed Tomography / Computed Tomography (SPECT/CT) is usually performed to ensure no significant irradiation of the lung or any other extrahepatic microspheres distribution, as well as to predict the post-therapeutic biodistribution of the microspheres in the tumor and in the normal liver. Furthermore, after the ^{90}Y microsphere SIRT, a ^{90}Y- Positron Emission Tomography / Computed Tomography (PET/CT) can be performed (due to the positron

emission of ^{90}Y) in order to make sure the ^{90}Y microspheres were distributed within the tumor. Both these acquisitions can be used for dosimetric calculations.

Suppliers of both glass and resin ^{90}Y microspheres suggest several methods, some based on the partition MIRD model, for the calculation of the needed activity in a specific dose. In the case of glass ^{90}Y microspheres, the suggested dose for the treated hepatic lobe usually ranges from 120 Gy to 150 Gy (depending on the treatment objective and the Child-Pugh status) and reaches 190 Gy for a segmentectomy [2]. The lobar mass is estimated based on morphological imaging [1] as a volume and then multiplied by a fixed density value. Once the activity to be administered has been set up, this value and the lung shunt measured on planar scintigraphy are used to estimate the dose absorbed by the lungs. If necessary, hepatic-not-tumoral-tissue dosimetry also can be estimated on PET/CT slices.

The personalized dosimetric approach is more and more popular, firstly because several recent studies have highlighted the need for a higher tumoral irradiation to be efficacious [3–5] while avoiding an over-irradiation of the lungs, other extra-hepatic tissues, and hepatic-not-tumoral-tissues; secondly because the estimation of the dose absorbed by tumoral and non-tumoral tissues has been made possible by several commercially available software. This software can perform segmentation and coregistration of functional and morphological imaging based on artificial intelligence.

Although several recommendations have been made to avoid over-or under- irradiation during radionuclide therapy, and accumulating data about the treatment optimization after personalized dosimetry have become available [6], only a few studies have described the implementation of dosimetric software in clinical routine protocols [4, 7–11]. Furthermore, only a small part of these studies uses commercially available software for the internal dose estimation of the tumoral, lobar, or whole liver absorbed doses based on SPECT/CT and/or PET/CT [4,8, 9]. The first aim of the present study was to compare two dosimetric approaches based on SPECT/CT and PET/CT data, using Simplicit^{90}Y™ vers. 2.1 (a commercially available software for dosimetric purposes in SIRT) *versus* the supplier suggested method for activity calculation. A second aim constituted in the investigation of a relation between dosimetric parameters and overall survival.

2. Material and methods

2.1. Patients

All procedures were performed in compliance with relevant laws and institutional guidelines, informed consent was obtained for each patient and this study was approved by the local Institutional Review Board.

A total of 19 successive patients, with a median age of 63.1 years (46–77 years), were included in this retrospective observational study from June 2016 to July 2019. Among them, 15 were treated for HCC, 2 for liver metastases of colorectal cancer and 2 for intra hepatic cholangiocarcinoma. Overall, 21 SIRT procedures were performed (procedure performed twice for 2 patients), (see Table 1 for patients' clinical characteristics and treatments' features). All patient data were discussed in a multidisciplinary team meeting

specialized in liver malignancies and including liver surgeons, and their tumors were considered as non-resectable, therefore SIRT was the chosen treatment option.

Each patient, before SIRT, underwent 4-phases contrast-enhanced (ce) CT or ce MRI to prepare angiography and estimate the lobar volume. A baseline angiography was performed by the same radiologist during the work-up phase and during SIRT. Before each procedure, biological parameters as coagulation testing and liver function tests were assessed (Table 1).

During the treatment planning, digital subtraction angiography was performed to identify the vessels supplying the tumor and coil-embolize others in order to avoid the deposition of the radioembolic microspheres to extrahepatic organs, according to international recommendations [12]. Cone Beam CT was not available.

2.2. Work up, SIRT procedure, SPECT and PET acquisition

At the end of the digital subtraction angiography, approximately 185 MBq of ^{99m}Tc-macroaggregated albumin was injected according to standard guidelines [1] in the selected hepatic lobe to assess the pulmonary shunt and detect digestive uptake if any. Planar acquisitions were performed in a Symbia T2, Siemens for lung shunt evaluation. SPECT/CT acquisitions were conducted with the following parameters: window, 140 ± 7.5 keV; 32 projections; 180°; matrix, 128 × 128; and 10 s/projection. Images were reconstructed with attenuation correction using a CT attenuation map. The images were analyzed as for current scintigraphy. None of the treated patient developed radiation-induced pneumonitis or extrahepatic radiation-induced disease.

The SIRT procedure was performed 14–21 days later, after another angiography, executed by the same radiologist, with ^{90}Y glass matrix embedded microspheres (Theraspheres® BTG Interventional Medicine). In order to calculate the injected activity, the planned absorbed dose of the perfused hepatic volume was 120 Gy for all patients (except in 4 cases for which clinical reasons led to a reduction of the aimed dose, Table 1), without exceeding 30 Gy to the lungs. The activity to be administered was calculated according the formula provided by the supplier:

$$A = \text{Dose}(120\,\text{Gy}) \times 50 \times (1 - \text{Lung Shunt})/\text{perfused liver mass}$$

where the perfused liver mass was determined on the pretreatment morphological imaging using the classification of Couinaud for liver segmentation. Retrospectively, the absorbed dose was estimated from SPECT data for the imaging aided dosimetry [2]. After the SIRT procedure, all patients underwent scanning using the Discovery 710 PET/CT system General Electric (GE Healthcare, Waukesha, WI, USA). Patient workup included liver focalized abdominal CT scan during free breathing. Then, a 3-dimensional PET scan (emission data, 6 min per bed position, 2 bed positions) was performed. Each examination was performed as soon as possible after the SIRT injection and always <1 h.

2.3. Simplicit90Y™ running

Simplicit90Y™, a dosimetry software, was used to co-register all the scans and to estimate the absorbed dose according to the SPECT and PET microspheres distribution. To perform

the dosimetry determination, the functional images were co-registered on anatomical volumes (CT/MRI) to determine the absorbed dose by the tumor, the liver lobe and the whole liver. The image registration functionality of Simplicit90Y™ was used to superimpose anatomical and functional images: “rigid or deformable (elastic) option”. The absorbed dose was automatically determined by the software considering the “number of counts” of the functional imaging contained in the anatomical volume considered. Only rigid, automatic and manual co-registrations were used for further purposes as the deformable co-registration was considered as excessively deforming for SPECT and PET data. Simplicit90Y™ was used to estimate the tumoral, lobar (perfused volume) and whole liver absorbed dose as well as the overlap of biodistribution of microspheres from SPECT and PET imaging. The evaluated biodistribution was based on a threshold percentage (10 %, 20 %, and 40 %) of the maximum uptake on SPECT and PET. These thresholds were chosen arbitrarily, based on our experience. The entire process lasts roughly one hour.

2.4. Statistics

Given the small patients population, medians were compared using Wilcoxon paired test or Mann-Whitney test according to analysis (paired or not paired test respectively). The overlap in distribution volumes of microspheres between PET and SPECT, or between the morphological tumor volume (on CT or MRI) and the functional volume (PET or SPECT), were estimated with the the Sørensen Dice Index (SDI) for three different cut-offs: 10 %, 20 % and 40 % of the maximal uptake. Cox proportional hazard regression, ROC curves, and Kaplan Meier survival analysis were used in order to explore the relation between SIRT and overall survival. MedCalc 18.2 Software, Mariakerke, Belgium was used for all purposes with a cut-off p-value of 0.05.

3. Results

3.1. Overlap between SPECT and PET

The median biodistribution volume was estimated for SPECT to 652.4 mL, 323.0 mL, and 53.9 mL with a 10 %, 20 %, and 40 % threshold, respectively. The median biodistribution volume was estimated for PET to 707.4 mL, 284.0 mL, and 58.0 mL with a 10 %, 20 % and 40 % threshold, respectively. The intersection of the SPECT and PET biodistributions were 481.1 mL, 140.5 mL, and 6.5 mL with a 10 %, 20 % and 40 % threshold, respectively (Table 2). This overlap between the PET and SPECT biodistributions, on absolute value as well as on SDI, was highly dependent on cut-offs. The overlap was significantly higher for the intersection at 10 % compared to both the intersection at 20 % ($p < 0.0001$) and 40 % ($p < 0.0001$), and significantly higher for the intersection at 20 % compared to the intersection at 40 % ($p < 0.0001$), Fig. 1A.

3.2. Overlap between morphological and functional imaging

The median and mean (± SD) tumor volume estimated from the morphological imaging were 114.1 mL and 291.2 mL (± 423.2), respectively. The median, mean, and SD of overlap between the functional imaging (both ^{99m}Tc-MAA and ^{90}Y-Microspheres) biodistribution and the tumor volume estimated from the morphological imaging for each threshold are presented in Table 3, as well as in Fig. 1B and C. The overlap was considered suboptimal for

small volume (<50 mL) infiltrated tumors. In other words, the overlap for tumor volumes > 50 mL was significantly higher (for Mann-Whitney tests of SDI for cut-offs 10 % and 20 %) than for tumor volumes < 50 mL.

3.3. Predicted and real irradiation of tumor and whole liver estimated with Simplicit90Y™

The median and mean (± SD) dose absorbed by the tumor estimated based on PET imaging were 129.7 Gy and 121.7 Gy (± 50.0), which was not significantly different from 116.8 Gy and 130.3 Gy (± 75.5) when estimated based on SPECT imaging (p = 0.50).

The median and mean (± SD) dose absorbed by the whole liver estimated based on PET imaging were 44.6 Gy and 44.2 Gy (± 19.6), which was not significantly different from 43.8 Gy and 44.6 Gy (± 18.7) when estimated based on SPECT imaging (p = 0.45).

3.4. Irradiation and volume of the perfused lobe, Simplicit90Y™ versus supplier recommendations

The median and mean (± SD) of perfused lobe absorbed dose estimated with Simplicit^{90}Y™ from PET imaging were 97.7 Gy and 95.5 Gy (± 19.7), which were significantly lower than 113.7 Gy and 109.9 Gy (± 16.0) when estimated with the conventional supplier suggested method (p = 0.004), Fig. 2. The median and mean (± SD) of perfused volume estimated from PET imaging were 1110.0 mL and 1239.9 mL (± 491.4), which was significantly higher than the median and mean (± SD) lobar perfused volume estimated from morphological imaging (940.0 mL and 1045.5 mL (± 494.7); p = 0.0002).

3.5. Prognosis, tumoral dosimetry, and tumoral overlap

The prognostic data tested for each patient was overall survival. Tested parameters were tumor dosimetry and tumor overlap after the administration of ^{90}Y microspheres as observed on ^{90}Y PET/CT. The Cox multivariate regression showed a significant relation (overall model fit, p = 0.0033) when covariates such as tumoral dosimetry (based on ^{90}Y PET/CT) as well as SDI between morphological tumoral distribution and ^{90}Y microspheres distribution (as observed on PET/CT), with percentage isocontour at 40 %, were used. The Cox regression hazard was modeled as:

$$H(t) = H_0(t) \times \exp[(-13.6121 \times \text{SDI TY40}) + (-0.0013 \times \text{Tum Dos})]$$

H(t) = The probability of death at each time point

H0(t) = The probability of death at baseline

SDI TY40 = SDI between the morphological tumoral distribution and ^{90}Y microspheres as observed on ^{90}Y PET/CT with isocontour at 40 %

Tum Dos = Tumoral Dosimetry expressed in Gray as measured on Simplicit90Y™.

The cumulative hazard according to Cox multivariate regression was estimated for each patient, and was then dichotomized according to the ROC curve. Finally, the cumulative hazard was used as factor codes of the Kaplan Meier survival analysis. The cumulative hazard (according Cox multivariate regression, based on SDI between morphological tumoral distribution and ^{90}Y microspheres as observed on PET/CT with isocontour at 40 % and tumoral dosimetry) was significantly related to the overall survival ($p = 0.0089$). The Kaplan Meier survival analysis allowed a statistically significant dichotomization between patients with higher survival compared to those with a shorter one (Figs. 3,4).

4. Discussion

More and more precision on dosimetric evaluations and reporting are required from nuclear medicine practice, in particular when radionuclide therapy is proposed [13]. The present work has been undertaken in this context, with the aim of exploring and improving the dosimetric aspects of the use of SIRT in clinical routine. As the availability of commercial software helps in performing easier dosimetric evaluations, the practice of SIRT should gain in precision and accuracy in the near future, especially with the voxel-based dosimetric analysis, the process automation by artificial intelligence for co-registration among the different types of imaging, and the segmentation of volumes of interest.

In the present study, the differences in biodistribution of ^{99}Tc-MAA and ^{90}Y Glass Microspheres after Simplicit90Y™ running were estimated and compared to the suggested supplier method. Overall, the predicted doses absorbed by the tumor or the whole liver were not significantly different from the absorbed doses estimated after SIRT.

Importantly, the overlap between the ^{99m}Tc-MAA biodistribution and the ^{90}Y Glass Microspheres biodistribution was far from perfect after Simplicit90Y™ running. In fact, with a good overlap, a SDI increasing with an increase of the threshold would be expected, and the opposite effect was observed herein. This mismatch between biodistributions has been previously reported [4,14–16], and is probably due to the manipulation of catheter positioning and/or dimensions of the microspheres, among other parameters. However, these differences did not have a significant impact on dosimetric calculations. An optimization in the organizational field (same patient positioning, fixed table targets, respiratory gating, iodine contrast enhancement, and same catheter position followed by a homogenous injection of the microspheres) should help in ensuring a better co-registration between functional and morphologic images, and between ^{99m}Tc-MAA scintigraphy and ^{90}Y bounded microspheres PET.

There was a significant difference between the estimations of the dose absorbed by the treated lobe depending on the method used (supplier suggested method or Simplicit90Y™ running), which could at least partially be due to the volumes considered for the estimations. EANM Guidelines recommend the use of morphological imaging for the estimation of the volume [1], which is easier, while other studies used functional imaging to estimate the volume of distribution of ^{90}Y microspheres [3], which provides a more precise dose to the irradiated tumor. From an internal dosimetry point of view, the later approach seems more correct. Overall, differences in volume estimation seem to induce differences in dosimetry,

fixing this issue should be aided by the increasing availability of voxel-based dosimetry software using artificial intelligence.

Consistently with previously published data [17–20], the present study revealed a significant relation between the tumoral dosimetry and the tumoral overlap by ^{90}Y microspheres on the one hand, and overall survival on the other hand. The tumoral dosimetry was estimated by Simplicit90Y™, avoiding deformable co-registration. Then, the same software allowed the estimation of the overlap between the tumoral distribution according to the morphologic imaging (CT or MRI) and the volume of the most intense ^{90}Y microspheres biodistribution, according to ^{90}Y PET/CT after spheres administration. Both the tumor dose and tumor overlap with ^{90}Y microspheres biodistribution were significantly correlated with the overall survival predicting the death probability for each patient. The Kaplan Meier curves confirmed the significant dichotomization of the patients based on survival probability, paving the way in our center to the use of dosimetry by voxel-based imaging.

To date, only a few studies have used voxel-based dosimetry software. Recently, Hermann et al. showed the beneficial impact of higher tumor radiation absorbed dose based on ^{99m}Tc-MAA SPECT/CT using the software MITK Workbench [20], while Levillain et al. used Planet Onco 3.0 Dosisoft to estimate the tumor received dose after SIRT in order to predict the tumor response evaluated by FDG-PET/CT in metastatic colorectal cancer patients [9]. Although the latter results are encouraging, they still require further confirmation as the population studied was small and more than half of the lesions had to be excluded because of their small dimensions (<2 cm of diameter). This consideration seems in agreement with our observation of the mismatch between morphological and functionnal imaging for lesions smaller than 50 mL, pointing out the challenge to estimate correct dosimetry for small lesions.

Chiesa et al. used the STRATOS module (from Philips), but it had to be used in an IMALYTICS workstation in order to perform voxel-based dosimetry estimations [4], while Gnesin et al. used the PMOD software to estimate the agreement between predicted dosimetry based on ^{99m}Tc-MAA SPECT/CT and real dosimetry after SIRT based on ^{90}Y PET/CT, and found a good agreement [11]. Moreover, other institutions developed different approaches such as the use of a graphical user interface based on MATLAB (OEDIPE) for a personalized Monte Carlo dosimetry, recommending higher activity to be administered compared to the traditional model in patients undergoing SIRT. Compared to others studies for which the computing time was scaled in hours [19], the method presented herein could be completed in roughly one hour. Another approach was chosen by Wang et al. using an External Beam Radiation Therapy (EBRT) software to estimate internal dosimetry after SIRT in a combined management of patients treated sequentially with SIRT and EBRT, their approach was feasible but not yet externally validated [10].

The present study suffers from several limitations, including its retrospective design, the small study sample, and the heterogeneity in the previous treatments administered to each patient. Also, the thresholds for SPECT/CT and PET/CT were chosen arbitrarily. Moreover, it was unfortunately not possible to compare these data with another voxel-based dosimetry software.

In conclusion, ^{90}Y PET/CT after treatment seemed mandatory to estimate the actual absorbed dose by the tumor or the treated lobe, given the far from the perfect overlap between the ^{99m}Tc-MAA biodistribution and the ^{90}Y Glass Microspheres biodistribution. Another concern raised in the present study was the differences in dose calculation of the treated lobe estimated by the supplier package method *versus* using Simplicit90Y™, which can pave the way to further analyses about the kind of technique (functional imaging *versus* morphological imaging) that should be used to define the volume of the treated lobe. Finally, a relation between the tumoral dosimetry and the prognosis was suggested despite the small population, requiring further efforts to explore and to improve the impact of SIRT in treated patients.

Supplementary Material

Refer to Web version on PubMed Central for supplementary material.

Acknowledgements

The authors would like to thank the DRCI of Hospices Civils de Lyon for their support in English revision and in particular Mrs Hélène Boyer PhD.

Funding

This research did not receive any specific grant from funding agencies in the public, commercial, or not-for-profit sectors.

Abbreviations:

SIRT	Selective Internal Radiation Therapy
^{99m}Tc-MAA	Macroaggregate of Albumin labelled by 99 metastable technetium
SPECT	Single Photon Emission Computed Tomography
CT	Computed Tomography
^{90}Y	Yttrium 90
PET	Positron Emission Tomography
HCC	HepatoCellular Carcinoma
MIRD	Medical Internal Radiation Dose
Gy	Gray
MBq	MegaBecquerel
keV	kilo electron Volt
SDI	Sørensen Dice Index
SD	Standard Deviation

EBRT	External Beam Radiation Therapy
CholangioCa	Cholangiocarcinoma
Previous MED RT	Previous radiation treatment of the mediastinum
NA	Not available
∩	Intersection
mL	milliliter
T	Tumor

References

[1]. Giammarile F, Bodei L, Chiesa C, et al. , EANM procedure guideline for the treatment of liver cancer and liver metastases with intra-arterial radioactive compounds, Eur. J. Nucl. Med. Mol. Imaging 38 (2011) 1393–1406, 10.1007/s00259-011-1812-2. [PubMed: 21494856]

[2]. Salem R, Padia SA, Lam M, et al. , Clinical and dosimetric considerations for Y90: recommendations from an international multidisciplinary working group, Eur. J. Nucl. Med. Mol. Imaging 46 (2019) 1695–1704, 10.1007/s00259-019-04340-5. [PubMed: 31098749]

[3]. Garin E, Lenoir L, Edeline J, et al. , Boosted selective internal radiation therapy with 90Y-loaded glass microspheres (B-SIRT) for hepatocellular carcinoma patients: a new personalized promising concept, Eur. J. Nucl. Med. Mol. Imaging 40 (2013) 1057–1068, 10.1007/s00259-013-2395-x. [PubMed: 23613103]

[4]. Chiesa C, Mira M, Maccauro M, et al. , Radioembolization of hepatocarcinoma with (90)Y glass microspheres: development of an individualized treatment planning strategy based on dosimetry and radiobiology, Eur. J. Nucl. Med. Mol. Imaging 42 (2015) 1718–1738, 10.1007/s00259-015-3068-8. [PubMed: 26112387]

[5]. Piasecki P, Narloch J, Brzozowski K, et al. , The Predictive Value of SPECT/CT imaging in colorectal liver metastases response after 90Y-radioembolization, PLoS One 13 (2018) e0200488, 10.1371/journal.pone.0200488. [PubMed: 29990342]

[6]. Hänscheid H, Canzi C, Eschner W, et al. , EANM Dosimetry Committee series on standard operational procedures for pre-therapeutic dosimetry II. Dosimetry prior to radioiodine therapy of benign thyroid diseases, Eur. J. Nucl. Med. Mol. Imaging 40 (2013) 1126–1134, 10.1007/s00259-013-2387-x. [PubMed: 23576099]

[7]. Petitguillaume A, Bernardini M, Broggio D, et al. , Fractionation protocol design for treatment planning optimization in SIRT using the OEDIPE software, Radioprotection 49 (2014) 283–288, 10.1051/radiopro/2014020.

[8]. Wissmeyer M, Delattre BM, Zaidi H, Terraz S, Ratib O, 90Yttrium PET/MR-based dosimetry after liver radioembolization (SIRT), Clin. Nucl. Med 40 (2015) 355–357, 10.1097/RLU.0000000000000713. [PubMed: 25674869]

[9]. Levillain H, Duran Derijckere I, Marin G, et al. , ^{90}Y-PET/CT-based dosimetry after selective internal radiation therapy predicts outcome in patients with liver metastases from colorectal cancer, EJNMMI Res. 8 (2018) 60, 10.1186/s13550-018-0419-z. [PubMed: 30006851]

[10]. Wang TH, Huang PI, Hu YW, et al. , Combined Yttrium-90 microsphere selective internal radiation therapy and external beam radiotherapy in patients with hepatocellular carcinoma: from clinical aspects to dosimetry, PLoS One 13 (2018) e0190098, 10.1371/journal.pone.0190098. [PubMed: 29293557]

[11]. Gnesin S, Canetti L, Adib S, et al. , Partition model-based 99mTc-MAA SPECT/CT predictive dosimetry compared with 90Y TOF PET/CT posttreatment dosimetry in radioembolization of hepatocellular carcinoma: a quantitative agreement comparison, J. Nucl. Med 57 (2016) 1672–1678, 10.2967/jnumed.116.173104. [PubMed: 27307346]

[12]. Salem R, Lewandowski RJ, Gates VL, et al. , Research reporting standards for radioembolization of hepatic malignancies, J. Vasc. Interv. Radiol 22 (2011) 265–278, 10.1016/j.jvir.2010.10.029. [PubMed: 21353979]

[13]. Lassmann M, Chiesa C, Flux G, Bardiès M, EANM Dosimetry Committee. EANM Dosimetry Committee guidance document: good practice of clinical dosimetry reporting, Eur. J. Nucl. Med. Mol. Imaging 38 (2011) 192–200, 10.1007/s00259-010-1549-3. [PubMed: 20799035]

[14]. Ulrich G, Dudeck O, Furth C, et al. , Predictive value of intratumoral 99mTc-macroaggregated albumin uptake in patients with colorectal liver metastases scheduled for radioembolization with 90Y-microspheres, J. Nucl. Med 54 (2013) 516–522, 10.2967/jnumed.112.112508. [PubMed: 23447653]

[15]. Chiesa C, Lambert B, Maccauro M, et al. , Pretreatment dosimetry in HCC radioembolization with (90)Y glass microspheres cannot Be invalidated with a bare visual evaluation of (99m)Tc-MAA uptake of colorectal metastases treated with resin microspheres, J. Nucl. Med 55 (2014) 1215–1216, 10.2967/jnumed.113.129361. [PubMed: 24898027]

[16]. Wondergem M, Smits ML, Elschot M, et al. , 99mTc-macroaggregated albumin poorly predicts the intrahepatic distribution of 90Y resin microspheres in hepatic radioembolization, J. Nucl. Med 54 (2013) 1294–1301, 10.2967/jnumed.112.117614. [PubMed: 23749996]

[17]. Garin E, Rolland Y, Edeline J, ^{90}Y-loaded microsphere SIRT of HCC patients with portal vein thrombosis: high clinical impact of 99mTc-MAA SPECT/CT-Based dosimetry, Semin. Nucl. Med 49 (2019) 218–226, 10.1053/j.semnuclmed.2019.01.006. [PubMed: 30954188]

[18]. Badiyan S, Bhooshan N, Chuong MD, et al. , Correlation of radiation dose and activity with clinical outcomes in metastatic colorectal cancer after selective internal radiation therapy using yttrium-90 resin microspheres, Nucl. Med. Commun 39 (2018) 915–920, 10.1097/MNM.0000000000000887. [PubMed: 30124600]

[19]. Petitguillaume A, Bernardini M, Hadid L, de Labriolle-Vaylet C, Franck D, Desbrée A, Three-dimensional personalized Monte Carlo dosimetry in 90Y resin microspheres therapy of hepatic metastases: nontumoral liver and lungs radiation protection considerations and treatment planning optimization, J. Nucl. Med 55 (2014) 405–413, 10.2967/jnumed.113.120444. [PubMed: 24504053]

[20]. Hermann AL, Dieudoné A, Ronot M, et al. , Relationship of tumor radiation-absorbed dose to survival and response in hepatocellular carcinoma treated with transarterial radioembolization with 90Y in the SARAH study, Radiology (2020) 191606, 10.1148/radiol.2020191606.

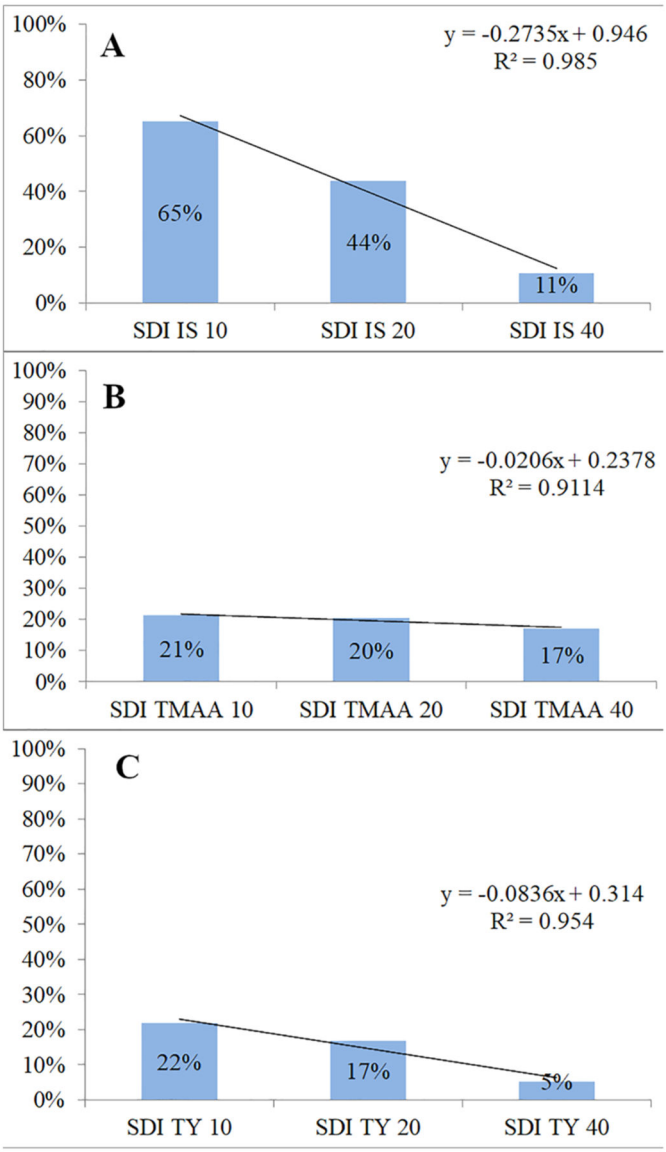

Fig. 1.

A: Median intersection between PET and SPECT for different thresholds measured as Sørensen Dice Index (SDI) with the function estimated by Microsoft® Excel®. B: Median intersection between morphological distribution of the tumor (CT or MRI) and SPECT for different thresholds measured as Sørensen Dice Index (SDI) with the function estimated by Microsoft® Excel®. C: Median intersection between morphological distribution of the tumor (CT or MRI) and PET for different thresholds measured as Sørensen Dice Index (SDI) with the function estimated by Microsoft® Excel®.

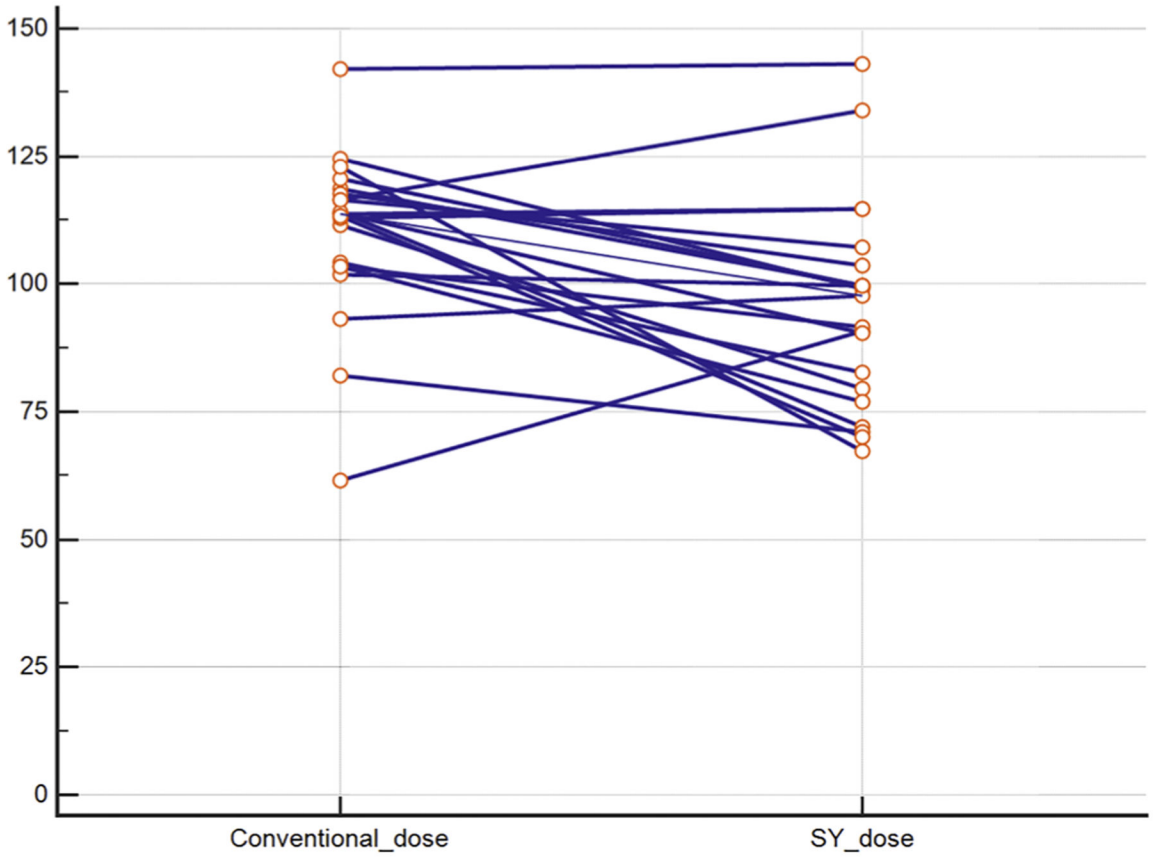

Fig. 2.

Case by case dosimetry for each patient according to conventional measured dose and according to Simplicit $^{90}Y^{TM}$ (SY) for each treated lobe.

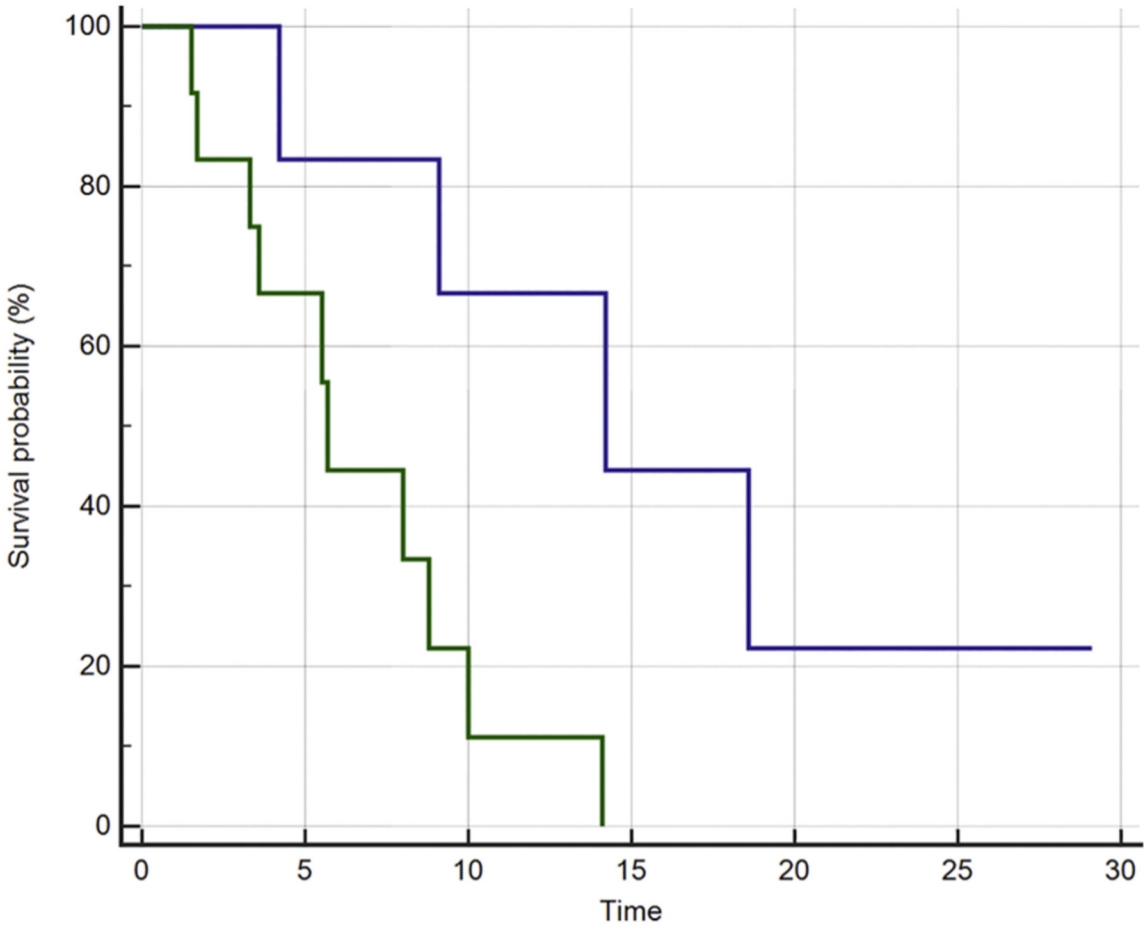

Fig. 3.

Kaplan-Meier survival curves based on the dichotomized Cox parameter (estimated according to Tumoral Dosimetry expressed in Gray as measured on Simplicit90Y™ and SDI between morphological tumoral distribution and ^{90}Y microspheres as observed on ^{90}Y PET/CT with isocontour at 40 %) for the two groups (higher survival in blue, shorter survival in green). (For interpretation of the references to colour in this figure legend, the reader is referred to the web version of this article).

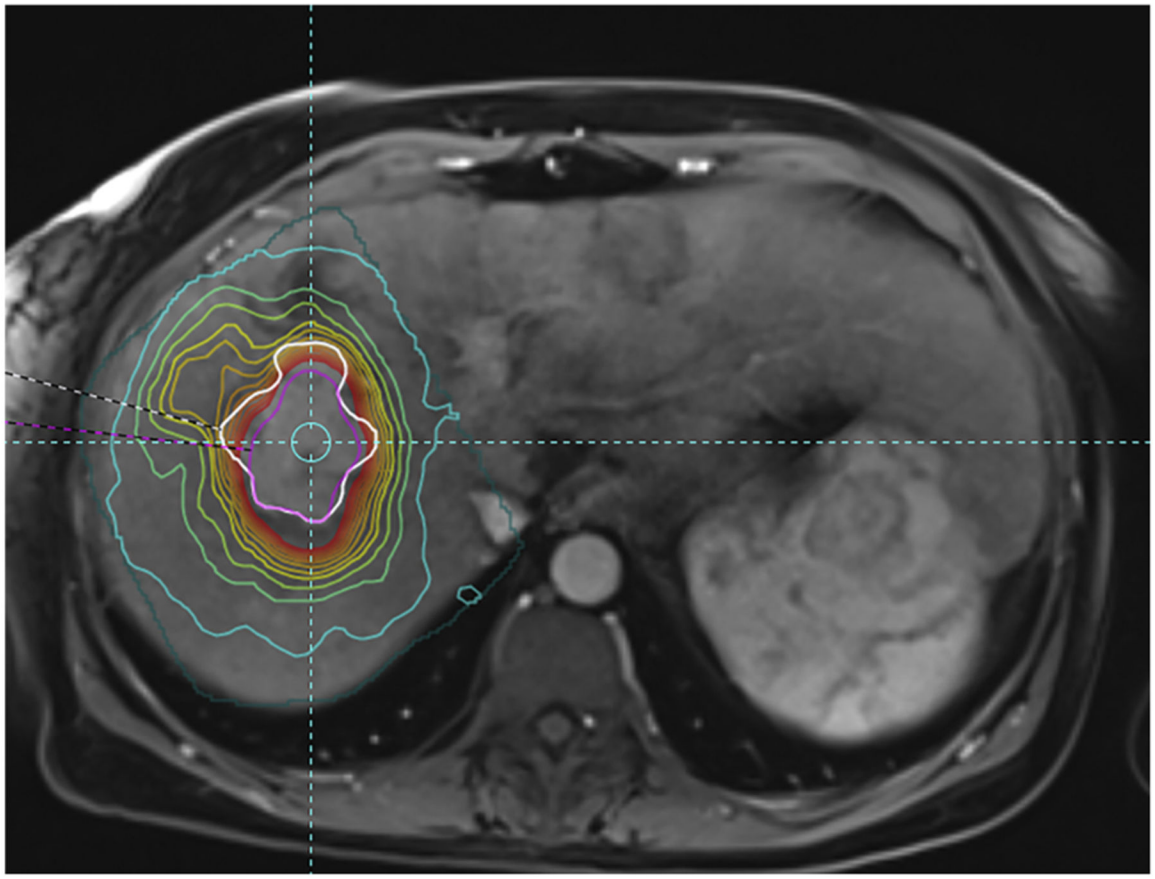

Fig. 4.

Axial slice showing arterial liver MRI image with tumoral segmentation (white line), intersection of the tumor with the 40 % isocontour of ^{90}Y microspheres biodistribution (pink line), of a 53 year-old woman (Pt 10) undergoing SIRT for a right lobe hepatocellular carcinoma (other colors show isodose lines according to Simplicit90Y™). She was alive at the last follow-up 29 months after SIRT, SDI TY 40 33.6 %, and Tumoral Dosimetry 101.2 Gy.

Biomed Pharmacother. Author manuscript; available in PMC 2022 May 10.

Table 1

Clinical characteristics of the overall population and technical features of the treatments.

Patient	SEX	AGE (Y)	DIAGNOSIS	n° LINE OF TRT	ECOG STATUS	CHILD-PUGH STATUS	TREATED LOBE	AIMED DOSE (Gy)	OTHER
1	F	68	Hepatic mets 1	4°	0	NA	Lobar Left	120	
2	M	63	CholangioCa	2°	0	B7	Lobar Left	80	
3	M	71	CholangioCa	1°	1	B7	Lobar Left + S4	80	Previous MED RT
4	F	58	Hepatic mets 2	4°	1	NA	Lobar Right − S4	120	
5	M	71	HCC	4°	0	A6	Lobar Right	120	
5	M	71	HCC	5°	0	A6	Lobar Left	120	
4	F	58	Hepatic mets 2	5°	1	NA	Lobar Left + S4	120	
6	M	54	HCC	1°	0	A5	Lobar Left + S4	120	
7	F	71	HCC	1°	1	A5	Lobar Right − S4	120	
8	M	68	HCC	2°	0	A6	Lobar Right − S4	120	
9	M	77	HCC	3°	0	A5	Lobar Right − S4	120	
10	F	53	HCC	5°	0	B7	Lobar Right	120	
11	M	63	HCC	3°	0	B7	Lobar Right	100	
12	M	68	HCC	1°	0	A5	Lobar Left + S4	120	
13	M	63	HCC	2°	0	B7	Lobar Right	120	
14	M	54	HCC	2°	0	B7	Lobar Right	120	
15	M	47	HCC	2°	0	A6	Lobar Left	120	
16	M	65	HCC	3°	0	A5	Lobar Right	80	Athrophic Left Lobe
17	M	71	HCC	2°	0	A6	Lobar Right	120	
18	M	60	HCC	1°	0	A6	Lobar Right − S4	120	
19	M	52	HCC	2°	0	A5	Lobar Right − S4	120	

F: Female, M: Male; Y: Years; Hepatic mets 1: Hepatic metastasis from Colorectal Cancer; Hepatic mets 2: Hepatic metastases from small bowel carcinoid; CholangioCa: Cholangiocarcinoma; HCC: Hepatocellular Carcinoma; n° Line of trt: Radioembolisation order in the different lines of treatment; Previous MED RT: Previous radiation treatment of the mediastinum; NA: Not available.

Table 2

Volume (in mL) of biodistribution estimated by SPECT and PET, intersection and Sørensen Dice Index (SDI) for different thresholds compared to maximal activity.

	SPECT			PET			Intersection			SDI		
	10 %	**20 %**	**40 %**	**10 %**	**20 %**	**40 %**	**10 %**	**20 %**	**40 %**	**10 %**	**20 %**	**40 %**
Median	652.4	323.0	53.9	707.4	284.0	58.0	481.1	140.5	6.5	65%	44 %	11 %
Mean	676.0	386.8	101.6	700.6	296.8	59.0	445.8	157.8	16.8	62%	41 %	14 %
SD	482.7	345.8	94.5	346.6	179.8	47.4	296.0	133.0	19.7	18%	21 %	12 %

Biomed Pharmacother. Author manuscript; available in PMC 2022 May 10.

Table 3

Volume (in mL) of the intersection (∩) between Macroaggregates of Albumine (MAA) and tumor (T) as well as between microspheres of ^{90}Yttrium and tumor (T) and Sørensen Dice Index (SDI) for different thresholds compared to maximal activity.

	SPECT			PET		
	T∩MAA10 %	**T∩MAA20 %**	**T∩MAA40 %**	**T∩Y10 %**	**T∩Y20 %**	**T∩Y40 %**
Median	52.5	41.9	19.1	58.0	33.0	5.3
Mean	204.4	144.9	45.3	175.1	96.4	27.6
SD	300.8	215.8	70.3	220.6	135.3	45.4
	SDI T∩MAA10 %	**SDI T∩MAA20 %**	**SDI T∩MAA40 %**	**SDI T∩Y10 %**	**SDI T∩Y20 %**	**SDI T∩Y40 %**
Median	21 %	20 %	17 %	22 %	17 %	5%
Mean	30 %	28 %	17 %	29 %	26 %	12 %
SD	25 %	22 %	13 %	23 %	21 %	13 %

Biomed Pharmacother. Author manuscript; available in PMC 2022 May 10.